# A New Possibility of the Generalized Two-Dimensional Correlation Spectroscopy. 2. Sample−Sample and Wavenumber−Wavenumber Correlations of Temperature-Dependent Near-Infrared Spectra of Oleic Acid in the Pure Liquid State

**Slobodan Šašić, Andrzej Muszynski, and Yukihiro Ozaki***

*Department of Chemistry, School of Science, Kwansei-Gakuin University, Uegahara, Nishinomiya 662-8501, Japan*

*Received: February 9, 2000; In Final Form: April 24, 2000*

This paper reports an example of the application of sample−sample correlation spectroscopy, the novel possibility of the generalized two-dimensional (2D) correlation spectroscopy, proposed in the preceding paper. Temperature-dependent near-infrared (NIR) spectral variations of oleic acid (*cis*-9-octadecenoic acid) in the pure liquid state have been analyzed in the region 7600−6600 $cm^{-1}$ by two kinds of 2D correlation analyses, wavenumber−wavenumber and sample−sample correlation. The analyses have been made for the NIR spectra after two kinds of different spectral pretreatments and also for the raw spectra. First, the spectra have been offseted on the higher wavenumber side (around 7500 $cm^{-1}$) and adjusted with respect to the intensity of the band at 7182 $cm^{-1}$ measured at 15 °C. In the second pretreatment both wavenumber sides (the 7600−7400 and 6700−6600 $cm^{-1}$) have been baseline corrected and only C−H combination bands and a band due to the first overtone of the monomer O−H group have been considered. In the last case the original spectra without any pretreatment have been analyzed. The 2D wavenumber−wavenumber cross-product matrices, i.e., synchronous spectra, show that for the first and second cases the spectral variations concentrate on the C−H and O−H bands. The newly proposed sample−sample correlation verifies convincingly the existence of two phase transition temperatures at 32 and 55 °C that are important in the process of monomerization of dimers of oleic acid. The analysis based upon the raw spectra gives the strongest evidence for these temperatures in the sample−sample correlation pattern.

## Introduction

In the preceding paper[1] we have proposed sample−sample correlation spectroscopy, a novel possibility of the generalized two-dimensional (2D) correlation spectroscopy. The new type of correlation is concerned with some sample features (e.g., concentration) unlike the original type of generalized 2D spectroscopy that deals only with spectral features.[2−12] We have demonstrated that the sample−sample correlation can reveal the concentration dynamic in a two-component spectral system through monitoring spectral changes at all wavenumber points investigated.[1] The first applications of the sample−sample correlation spectroscopy were carried out for an artificial spectral system consisting of only two bands and that involving precisely two chemical species with a number of bands. Regardless of the promising results reported in the preceding paper,[1] a question for applicability of the sample−sample correlation spectroscopy still remains because the model spectral system investigated is rather far from real spectral systems. Therefore, the second part of our studies was concerned with the sample−sample correlation analysis of a real chemical system.

Our intention was to choose an essentially two-component system, spectroscopically not simple but at the same time analyzed in detail by other physicochemical techniques. In this way we may be able to explore the possibility of the sample−sample correlation approach as an analytical tool and to compare results obtained by this method with those gained by other methods. For these reasons we have chosen temperature-dependent near-infrared (NIR) spectra of oleic acid in the pure liquid state.

On the basis of a number of spectroscopic and physicochemical studies, Iwahashi et al.[13−17] showed that oleic acid probably has three kinds of liquid structures depending on temperature. In the temperature range from the melting point (15 °C) to 30 °C, the liquid structure consists of clusters having a quasi-smectic liquid crystal structure, while the structure in the temperature range between 30 °C and 55 °C is composed of clusters with a less ordered structure. Above 55 °C oleic acid appears to be an isotropic liquid. These conclusions have been drawn from the studies of oleic acid by NIR,[14] differential scanning calorimetry (DSC),[13] density, viscosity, and self-diffusion.

In the NIR spectra, neat oleic acid shows strong bands at 8271, 7194, 7092, and 6993 $cm^{-1}$.[14] The band at 8271 $cm^{-1}$ is due to the second overtone of the $CH_2$ stretching mode, and the rest are assigned to combination modes of the CH vibrations. To clarify the effect of density change, all the bands of oleic acid are reduced by comparing the intensity of the band at 8271 $cm^{-1}$ at various temperatures with that of the same band at 15.2 °C that was used as a standard (15.2 °C is just below the melting point of the $\beta$-type crystal of oleic acid).[13] The spectra at various temperatures became almost identical with each other except for the wavelength region above 6990 $cm^{-1}$. The band at 6920 $cm^{-1}$ that is not observed below 15.2 °C is due to the first overtone of the OH stretching vibration of the monomer. The

* To whom correspodence should be addressed. Fax: +81-798-51-0914. E-mail: ozaki@kwansei.ac.jp.

10.1021/jp0005118 CCC: $19.00 © 2000 American Chemical Society
Published on Web 06/17/2000

intensity of this band increases as a function of temperature, giving good evidence that the acid dimer dissociates into the monomeric species even in the pure liquid state. In the plot of the absorbance at 6920 $cm^{-1}$ versus temperature, one can see two break points at 30 and at 55 °C.[14,16] All the conclusions regarding the liquid structure were reached from the intensity change of the band at 6920 $cm^{-1}$. However, the obtained temperature-dependent plots of the intensity did not always give convincing evidence for the existence of the two break points.[14,16]

The purpose of the present study is to demonstrate the potential of the new type of 2D correlation analysis, sample−sample correlation spectroscopy. We have applied the sample−sample correlation analysis to the above problem of oleic acid. The present study has employed the whole spectral region of 7600−6600 $cm^{-1}$, so that it may yield more unambiguous evidence for the break points. We have also used the widely accepted wavenumber−wavenumber correlation method for additional characterization of the hydrogen bonds and dissociation in neat oleic acid at different temperatures. The temperature-dependent NIR spectral variations of oleic acid offer very challenging possibilities; they are rather hard to analyze by conventional one-dimensional spectroscopy because of severe overlapping of many bands, combination of small spectral changes, and strong influence of physical factors such as the density change.

## Experimental Section

A sample of oleic acid of very high purity (greater than 99.9%) was supplied by Nippon Oil and Fats Co. (Amagasaki, Japan) and was used without further purification. The NIR spectra were recorded on a Nicolet Magna 760 FT-IR/NIR spectrophotometer equipped with an PbSe detector at a resolution of 4 $cm^{-1}$. To ensure an acceptable signal-to-noise ratio, we accumulated 512 scans. During the FT-NIR measurements, a glass cell of 1 cm thickness was used. The cell was inserted into a commercially available thermostated cell holder, and the temperature was controlled by circulating thermostated water. The temperature of the sample was measured by means of a digital thermometer (Anritsu HFT-50) dipped into the cell. This system guaranteed a temperature control and stability of ±0.1 °C.

All the calculations have been made by use of the software composed in our laboratory. The 2D correlation analyses have been carried out by both generalized 2D correlation spectroscopy methods proposed by Noda,[2] the wavenumber−wavenumber correlation and our extension of his proposal, the sample−sample correlation.[1] Before the calculation of the matrices is carried out, usually the spectral data are subjected to the mean normalization. When the wavenumber−wavenumber correlation is performed, every column of the experimental matrix, **M**, is divided by its mean value, while in the case of the sample−sample correlation every column of $\mathbf{M}^T$ is divided by its mean value. Also, the centering in the wavenumber−wavenumber correlation means that the mean spectrum is subtracted from each spectrum while the centering in the sample−sample correlation means that the mean value from all the rows of $\mathbf{M}^T$ (the number of rows is equal to the number of spectra) is subtracted from columns of $\mathbf{M}^T$ (the number of columns is equal to the wavenumber points).

## Results and Discussion

Figure 1A shows NIR spectra in the 7600−6600 $cm^{-1}$ region of oleic acid in the pure liquid state over a temperature range of 15−80 °C. The assignment of the observed bands is given in the Introduction. On the lower wavenumber side appears the strong influence of a broad band due to the hydrogen-bonded O−H group of dimers located around 5850 $cm^{-1}$. On the higher wavenumber side, the baseline increases with temperature as a consequence of the change in the density of the sample. The spectra in Figure 1A were pretreated in way similar to that used by Iwahashi et al.[14] First, we applied the offset at 7600 $cm^{-1}$ and then adjusted the intensity at 7188 $cm^{-1}$ of all the spectra to be the same as that in the spectrum recorded at 15 °C. The spectra after the correction are shown in Figure 1B.

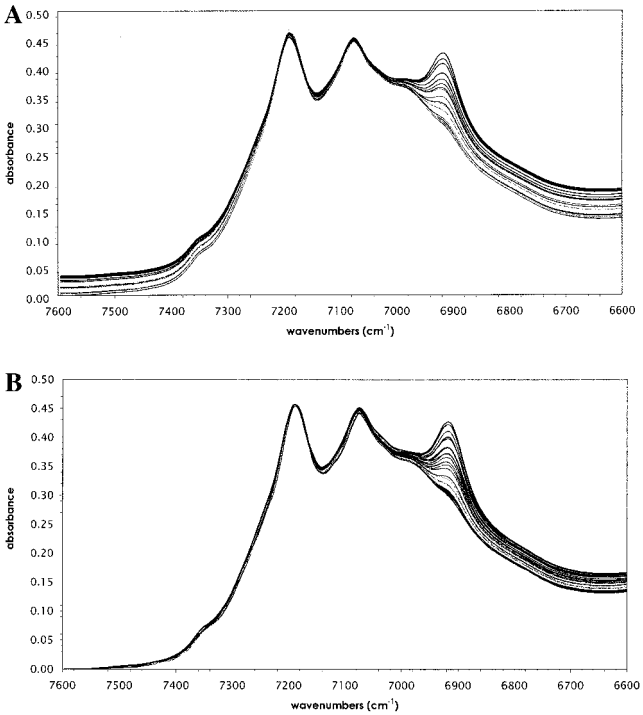


**Figure 1.** (A) NIR spectra in the region of 7600−6600 $cm^{-1}$ of oleic acid in the pure liquid state over a temperature range of 15−80 °C. (B) Spectra shown in Figure 1A after the offset at 7600 $cm^{-1}$ and adjusting the intensity at 7188 $cm^{-1}$ with respect to the spectrum recorded at 15 °C.

We have applied both the wavenumber−wavenumber correlation and sample−sample correlation analyses to the set of spectra in Figure 1B (total of 22 spectra). Since it seems that for the sample−sample correlation the correlation analysis after the mean normalization and centering gives more useful results for determining the concentration dynamics of species than the corresponding analysis without these pretreatments,[1] these two operations have been applied before the calculation of wavenumber−wavenumber correlation maps too.

In Figure 2A,B are shown wavenumber−wavenumber synchronous and asynchronous correlation spectra constructed from the temperature-dependent spectral variations of oleic acid. The synchronous spectral pattern is rather simple. It is dominated by a strong autopeak at 6917 $cm^{-1}$ that shows the negative correlation with the whole region of 7250−7020 $cm^{-1}$. The negative correlation of the band at 6917 $cm^{-1}$ with the spectral region where several C−H combination bands appear reveals that the band at 6917 $cm^{-1}$ increases with temperature while all the C−H bands have almost constant intensities. The asynchronous spectrum reveals a strong nonlinear relationship between the intensity change in the band at 6917 $cm^{-1}$ arising from the monomer and the intensity changes in the regions of 6600−6800 $cm^{-1}$ and 7000−7200 $cm^{-1}$ . The clear orthogonal correlation of the band at 6917 $cm^{-1}$ with other bands shows

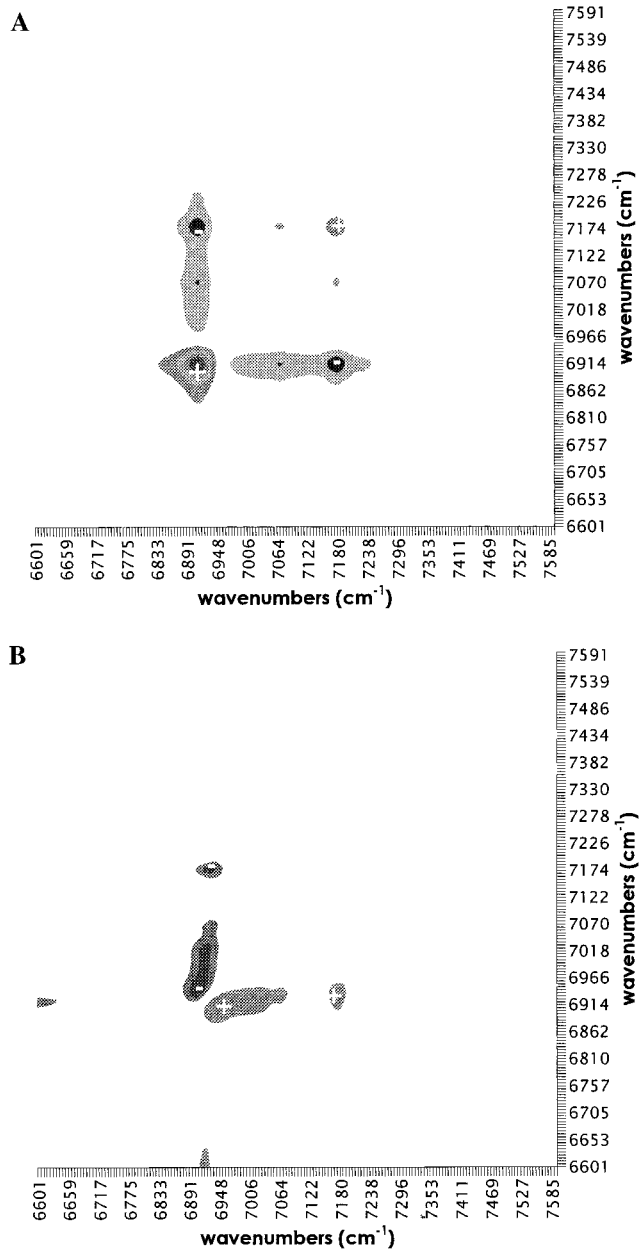


**Figure 2.** (A) Synchronous spectrum of the model shown in Figure 1B. (B) Asynchronous spectrum of the model shown in Figure 1B.

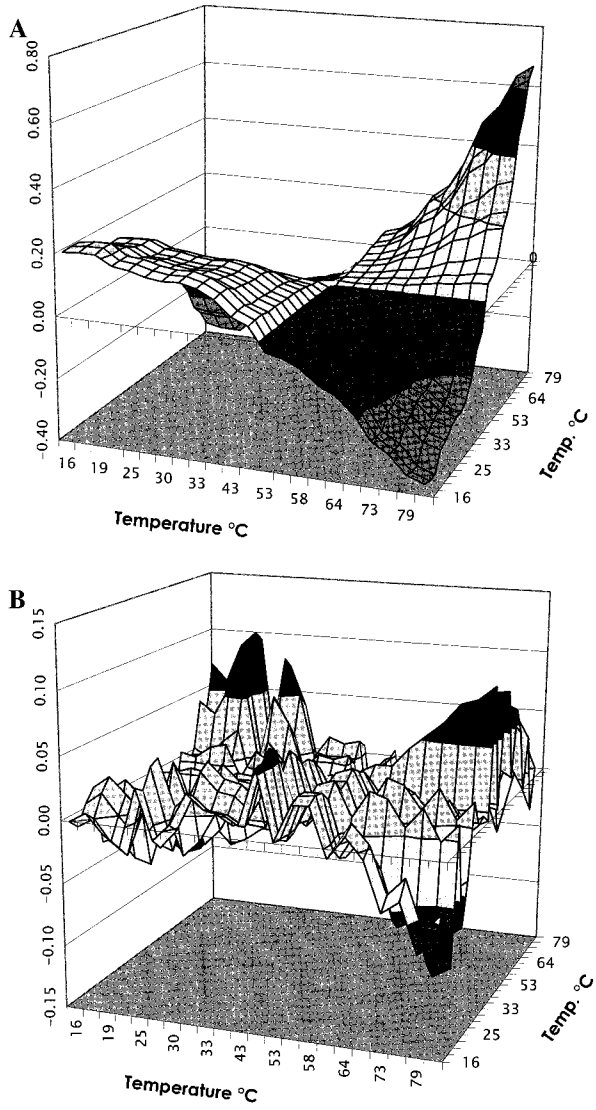


**Figure 3.** (A) Cross-product matrix (the synchronous spectrum) of the sample−sample correlation calculated from the spectra shown in Figure 1B. (B) Orthogonal cross-product matirx (the asynchronous spectrum) of the sample−sample correlation calculated from the spectra shown in Figure 1B.

the irregularity in the intensity change in the monomer O−H band. Since the 7600−6600 $cm^{-1}$ region is composed only of the static C−H bands and the variable O−H band of the monomer (Figure 1B), it seems that the temperature-dependent change of the monomer band is not linear through the whole temperature range. The negative correlation at 6903, 6930 $cm^{-1}$ suggesting the splitting of the band at 6917 $cm^{-1}$ but closeness of the band at 6990 $cm^{-1}$ and the pseudo-isosbestic point near 6950 $cm^{-1}$ might be reasons for that correlation too.

The covariance and orthogonal covariance matrices of the sample−sample correlation are shown in Figure 3A,B, respectively. In the present case the sample−sample correlation spectroscopy is the temperature−temperature correlation spectroscopy. The covariance matrix clearly shows that the concentration of the species in the lower temperature range decreases slowly up to 55 °C and above 55 °C a marked increase in the concentration of another species occurs. The orthogonal correlation (Figure 3B) shows that distinct nonproportionality in the rate of the concentration variation starts at ca. 55 °C and reaches the maximum at the temperature coordinate of (15, 80)°C. This suggests that the rate of dissociation is not uniform through the whole temperature range, but at least at one temperature some abrupt change happens. The asynchronous correlation spectrum is noisy due to small differences in the rates, but still one can observe the trend with the maximum at the temperature coordinate of (15, 80) °C.

The structural changes that take place at 32 and 55 °C are due to the phase transitions from the quasi smectic-liquid crystal to a more disordered liquid crystal and from the disordered liquid crystal to the isotropic liquid, respectively.[13] These changes are induced by monomer molecules that are present as impurities in oleic acid in the pure liquid state at room temperature. With the temperature increase the concentration of monomer increases and the transition to the disordered structure occurs. The population of the monomer is much smaller than that of the dimer even at 80 °C, but the existence of the monomer is of crucial importance for the process of monomerization.[14]

The major spectral change in the region of 7600−6600 $cm^{-1}$ is the intensity change in the O−H band of the monomer. There is no band in the above region directly connected with the

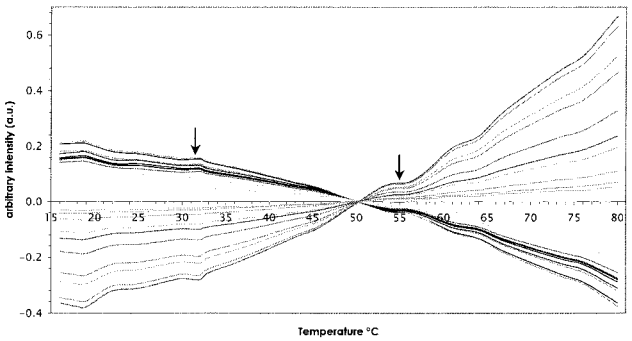


**Figure 4.** Series of slice spectra obtained from Figure 3A.

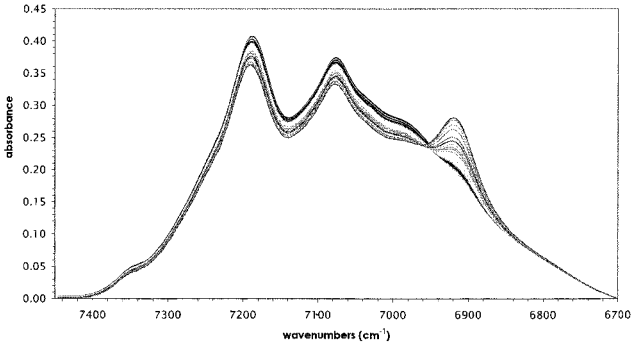


**Figure 5.** Spectra shown in Figure 1A after the baseline correction at both wavenumber sides.

dimers' concentration, but its concentration change could be monitored indirectly through the influence of the density change appearing in the whole spectral region and the influence of the strong dimer band located around 5800 $cm^{-1}$. It may also be monitored by the change in the concentration of the monomer because the only way of producing the monomer is the dissociation of the dimer.

We may be able to conclude from the synchronous spectrum in Figure 3A that the rate of conversion from the dimer into the monomers increases significantly after 55 °C. However, it is very hard to determine the exact temperature by the inspection of the map in Figure 3A. The three-dimensional representation does not offer a preview suitable for the analysis of details. Rather, we should concentrate our attention on the one-dimensional presentation, or slice spectra, of Figure 3A. Figure 4 exhibits the set of lines (slice spectra) that form the three-dimensional representation shown in Figure 3A. The pattern in Figure 3A is obtained by repeating any one of the lines in Figure 4 with intensity changes from sample to sample.[18,19] Thus, all the information obtained from Figure 4 is contained in Figure 3A too. One can see that at 55 °C all the slice spectra exhibit upward changes in the slopes. In this way we prove that the process of monomerization has at least two break points where the rate of monomerization is changed. However, the appearance of the break points at 32 and 55 °C will be demonstrated much more clearly later (see Figure 10B).

In the previous NIR studies the temperature of 32 °C was also noted as the first point where the transition from the quasi-smectic liquid crystal to the disordered liquid crystal occurs.[13] However, the evidence for the transition point at 32 °C was somewhat weak because the intensity change in the monomer O−H band is very small near 32 °C. Figure 4 suggests that 32 °C is the temperature where the monomerization of dimer starts to proceed faster. In the region of 15−30 °C there is almost no slope, showing that the monomerization process occurs little

We have undertaken additional pretreatment to eliminate the influence of the foot of the strong band around 5800 $cm^{-1}$ due to the dimer (not shown here). Figure 5 shows the NIR spectra in Figure 1A after the baseline correction in both wavenumber sides. By applying the baseline correction to both wavenumber sides, we have tried to focus our attention mainly on three major bands at 7189, 7076, and 6917 $cm^{-1}$. As can be seen from Figure 5, all spectral variations concentrate only on these three bands. The synchronous wavenumber−wavenumber correlation calculated after the mean normalization and centering is shown in Figure 6A. Note that the main 2D spectral features observed in Figure 2A again appear in Figure 6A. The strong autopeak at 6917 $cm^{-1}$ dominates, while the other two bands at 7189 and 7076 $cm^{-1}$ are noticed only through the negative correlation with the peak at 6917 $cm^{-1}$. The asynchronous correlation map

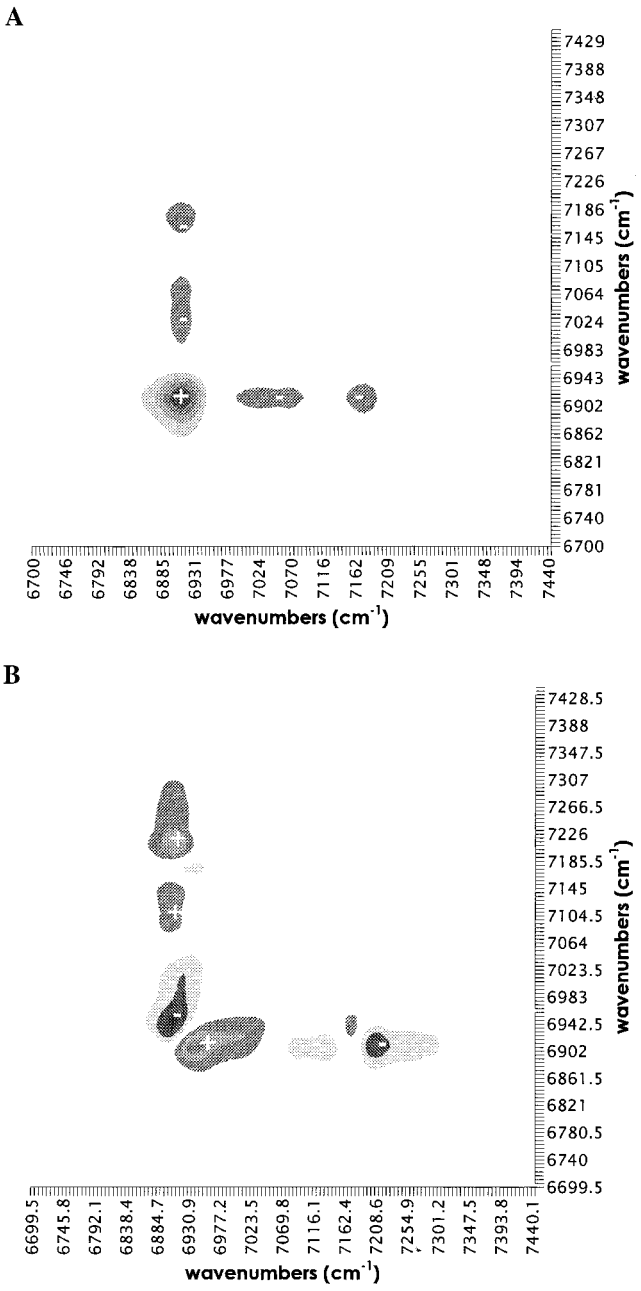


**Figure 6.** (A) Cross-product matrix of the spectra shown in Figure 5. (B) Orthogonal cross-product matrix of the spectra shown in Figure 5.

shown in Figure 6B is also similar to the correlation map shown in Figure 2B. It is very interesting that asynchronous cross-peaks again appear at nearly 6903, 6930 $cm^{-1}$. This observation

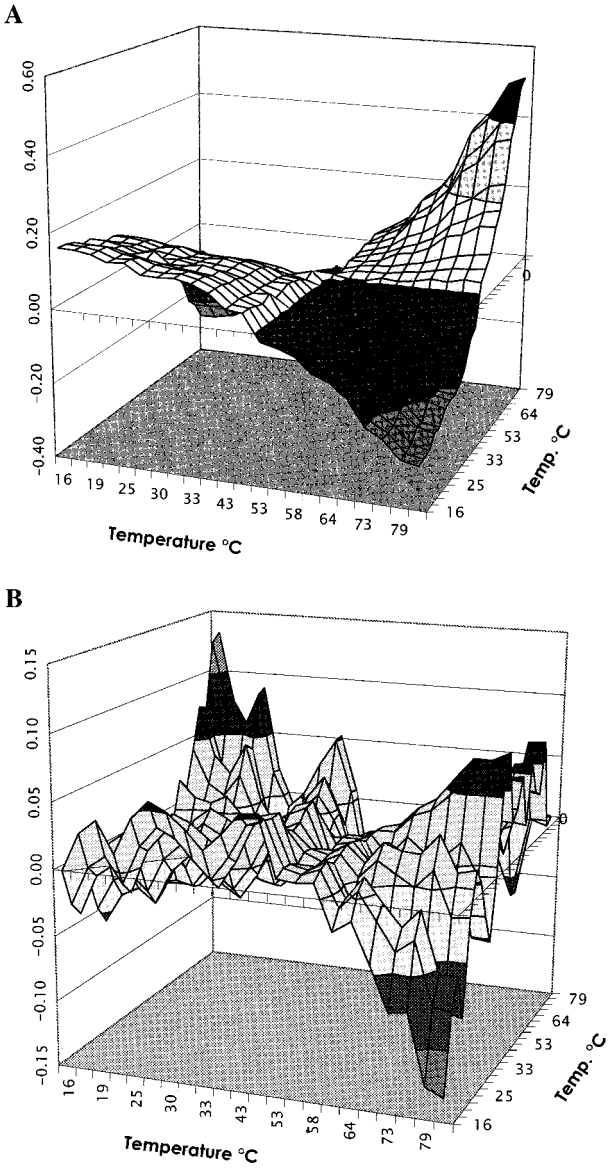


**Figure 7.** (A) Cross-product of the sample−sample correlation calculated from the spectra shown in Figure 5. (B) Orthogonal cross-product matrix calculated from the spectra shown in Figure 5.

strengthens our assumption about splitting of the band at 6917 $cm^{-1}$. In this spectral set we ignore the influence of the physical factors and hydrogen-bonded species. Therefore, the repeated correlation approximately at the same coordinate suggests even more strongly than in the previous case the possible appearance of the additional bands at 6903 and 6930 $cm^{-1}$. Moreover, the intensity change at 6903 $cm^{-1}$ is not evident in strict linear relationships with both C−H bands, as shown by the positive orthogonal correlation in Figure 6B.

In Figures 7A,B are shown covariance and orthogonal correlation matrices for the temperature range 15−80 °C. Figure 8 depicts the slice spectra. The main features in Figure 3A are reproduced in Figures 7A and 8, proving once more that the temperature of 55 °C is the break point where the slope becomes steeper. The orthogonal correlation shown in Figure 7B is very interesting. In comparison with Figure 3B, the noise is smaller and the orthogonal cross-peaks at the terminal temperatures appear clearly. This can be understood in exactly the same way as that in Figure 3B. The reason for the striking appearance of orthogonal correlation is the emphasis of the monomer O−H band by the baseline correction in the both wavenumber sides.

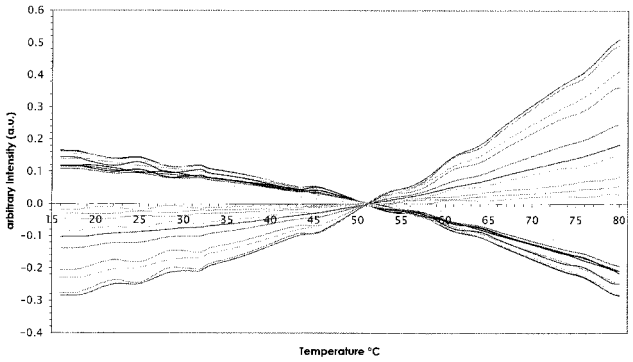


**Figure 8.** Slice spectra of the 3D presentation shown in Figure 7A.

Namely, in the previous set the influence of the dimer band was not removed and it obscured the monomer band, making the asynchronous spectra noisy. Now, the dominant part in the overall spectral variations is the monomer O−H band and the process of the monomerization can be followed easier in the orthogonal correlation than in the previous case.

Finally, we demonstrate the results of the correlation analysis of the raw spectra shown in Figure 1A. Parts A and B of Figure 9 present the synchronous and asynchronous wavenumber−wavenumber correlations generated from the spectra shown in Figure 1A. In the wavenumber−wavenumber correlation matrix (Figure 9A) one can find strong autopeaks at 7189 and 7076 $cm^{-1}$ and negative correlation of these peaks with the band at 6917 $cm^{-1}$ and with the region 7600−7300 $cm^{-1}$. The prominent appearances of the peaks due to the C−H combinations are expected because the pretreatments applied in the previous cases strongly suppress the spectral variances at their positions. The influence of the density change is very notable too. It is also totally excluded in the two previous trials. The asynchronous spectrum (Figure 9B) contains information mostly about the relations between the monomer O−H band and other spectral features.

There is a positive correlation between the band at 6917 $cm^{-1}$ and the whole region of 7600−7300 $cm^{-1}$ and negative correlations at 6917, 7186 and 6917, 7080 $cm^{-1}$. This indicates that the source of spectral variation in the band at 6917 $cm^{-1}$ is quite different from those in the C−H bands and those in the region of 7300−7700 $cm^{-1}$. However, the signs of the negative correlations should also be considered as positive here because the corresponding peaks in the synchronous spectrum have negative signs and, according to Noda's rule,[2] in such case the asynchronous cross-peaks change the sign.

Parts A and B of Figure 10 show a sample−sample covariance matrix generated from the spectra shown in Figure 1 and its slice spectra, respectively. Note that the slice spectra give rise to undoubted evidence for the two break points at 32 and 55 °C.

The correlation patterns in Figure 10A,B can be understood as follows. The spectra without any baseline correction, just after mean normalization and centering, emphasize the spectral variations through the whole region. Therefore, the spectral evidence for the phase transition of oleic acid based on the intensity change of the band at 6917 $cm^{-1}$ becomes less significant compared with the evidence from the rest of the spectra. In other words, we diminish information about the dissociation of the dimer, since only the band at 6917 $cm^{-1}$ is strongly connected with the specific species (monomer). By suppressing the importance of that band, we can hardly follow the rate of monomerization. In the present analysis the changes in the physical properties of oleic acid become important. The

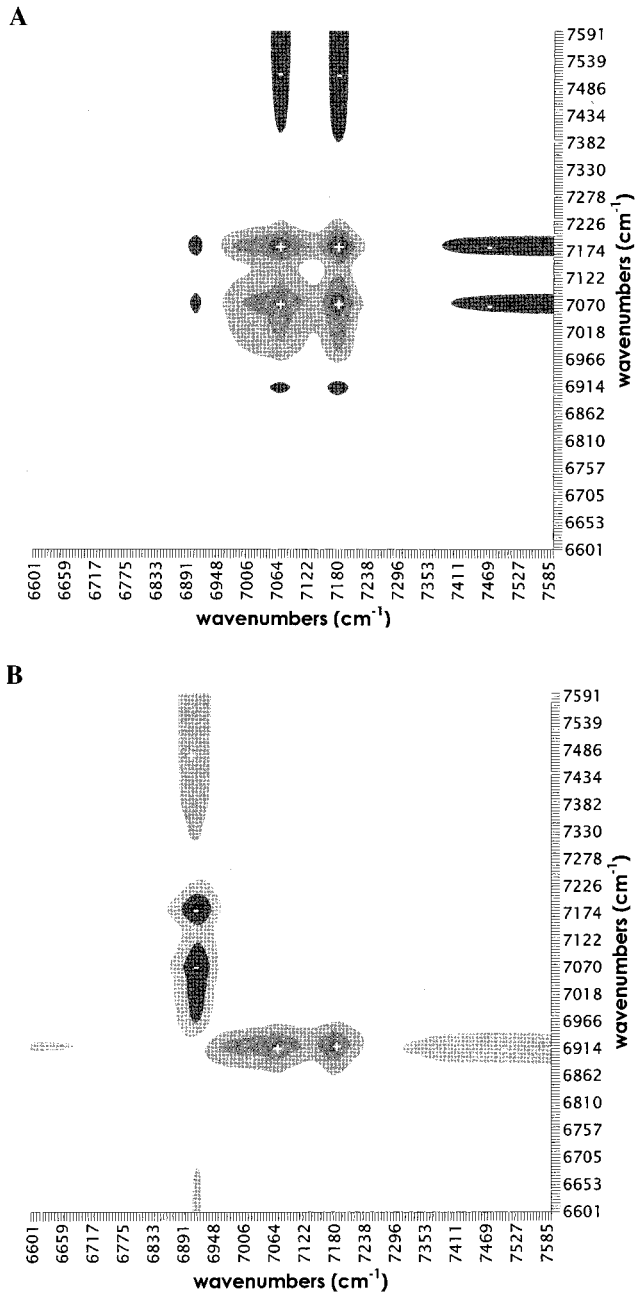


**Figure 9.** (A) Cross-product matrix calculated from the spectra shown in Figure 1A. (B) Orthogonal cross-product matrix calculated from the spectra shown in Figure 1A.

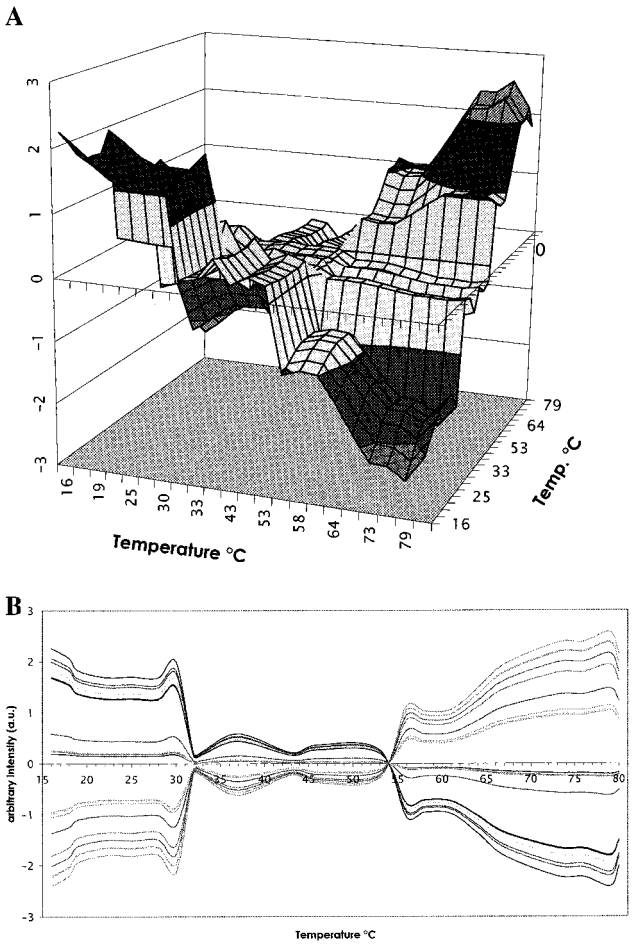


**Figure 10.** (A) Cross-product matrix of the sample−sample correlation calculated from the spectra shown in Figure 1A. (B) Slice spectra of the 3D representation shown in Figure 10A.

correlation patterns in these figures are created mostly by the spectral features in the region of 7600−6950 $cm^{-1}$. In this region all the spectral dynamics is governed by the temperature-dependent density change and changes in other physical properties of the sample. Therefore, the only way to understand Figure 10 is by distinguishing the three kinds of liquid structures for the temperature ranges 15−32, 32−55, and 55−80 °C. The present results are in good agreement with those of other physicochemical experiments such as the DSC measurements, viscosity, and self-difusion coefficient.[13]

## Conclusions

This paper has demonstrated that two types of correlation analysis are quite powerful in the analyses of temperature-dependent NIR spectral variations of oleic acid in the pure liquid state. We have tried three procedures to generate wavenumber−wavenumber and sample−sample correlation spectra. First, the analysis of the spectra that are offset on the higher wavenumber side shows that all spectral variances concentrate on the positions of major bands at 7194, 7092, and 6993 $cm^{-1}$. The asynchronous spectrum suggests the splitting of the monomer O−H band into two bands at 6902 and 6930 $cm^{-1}$. The corresponding sample−sample correlation analysis reveals the existence of two phase transition temperatures. Both temperatures are identified in the one-dimensional pattern of column cross-product matrices with the different number of spectra included in the calculation. The similar results are obtained when the only C−H and O−H bands are treated by excluding the strong effect of the density fluctuation and the interference from the intense dimer band near 5800 $cm^{-1}$. Finally, the raw spectra have been analyzed. The wavenumber−wavenumber correlation highlights the band at 6917 $cm^{-1}$ to have a different dynamics compared with the other wavenumber points. The sample−sample correlation of the raw spectra elucidates very convincingly the two phase transition temperatures.

The sample−sample correlation can be easily understood and applied to the systems where the process similar to the monomerization of dimer takes place. Since this method is just another aspect of generalized 2D correlation spectroscopy, all the advantages and limitations of the generalized 2D methodology are preserved in the sample−sample correlation. Therefore, the method is not restricted to this kind of perturbation: the same approach is valid for monitoring concentration changes of species with time, pressure, etc.

**Acknowledgment.** The authors thank Dr. M. Suzuki (Kyushu University) for preparing highly purified oleic acid and N. Yokochi (Kwansei-Gakuin University) for measuring NIR spectra of oleic acid.

## References and Notes

(1) Šašić, S.; Muszynski, A.; Ozaki, Y. *J. Phys. Chem. A* **2000**, *104*, 6380.

(2) Noda, I. *Appl. Spectrosc.* **1993**, *47*, 1329.

(3) Noda, I. *Appl. Spectrosc.*, in press.

(4) Noda, I.; Liu, Y.; Ozaki, Y. *J. Phys. Chem.* **1996**, *100*, 8665.

(5) Ozaki, Y.; Liu, Y.; Noda, I. *Macromolecules* **1997**, *30*, 2391.

(6) Czarnecki, M. A.; Maeda, H.; Ozaki, Y.; Suzuki, M.; Iwahashi, M. *J. Phys. Chem. A* **1998**, *102*, 9117.

(7) Ren, Y.; Shimoyama, M.; Ninomiya, T.; Matsukawa, K.; Inoue, H.; Noda, I.; Ozaki, Y. *J. Phys. Chem. B* **1999**, *103*, 6475.

(8) Wang, Y.; Murayama, K.; Myojo, Y.; Tsenkova, R.; Hayashi, N.; Ozaki, Y. *J. Phys. Chem. B* **1998**, *102*, 6655.

(9) Nabet, A.; Pezolet, M. *Appl. Spectrosc.* **1997**, *51*, 466.

(10) Gadaleta, S. J.; Gericke, A.; Boskey A. L.; Mendelsohn, R. *Biospectroscopy* **1996**, *2*, 353.

(11) Czarnecki, M. A.; Wu P.; Siesler H. W. *Chem. Phys. Lett.* **1998**, *283*, 326.

(12) Sefara, N. L.; Richardson, H. H. *Appl. Spectrosc.* **1997**, *51*, 536.

(13) Iwahashi, M.; Yamaguchi, Y.; Kato, T.; Horiuchi, T.; Sakurai, I.; Suzuki, M.; *J. Phys. Chem.* **1991**, *95*, 445.

(14) Iwahashi, M.; Hachiya, N.; Hayashi, Y.; Matsuzawa, H.; Suzuki, M.; Fujimoto, Y.; Ozaki, Y. *J. Phys. Chem.* **1993**, *97*, 3129.

(15) Iwahashi, M.; Hayashi, Y.; Hachiya, N.; Matsuzawa, H.; Kobayashi, H. *J. Chem. Soc., Faraday Trans.* **1993**, *89*, 707.

(16) Iwahashi, M.; Suzuki, M.; Czarnecki, M. A.; Liu, Y.; Ozaki, Y.; *J. Chem. Soc., Faraday Trans.* **1995**, *91*, 697.

(17) Czarnecki, M. A.; Czarnecka, M.; Ozaki, Y. Iwahashi, M. *Spectrochim. Acta* **1994**, *50A*, 1521.

(18) Šašić, S.; Muszynski, A.; Ozaki, Y. Submitted to *J. Phys. Chem.*

(19) Šašić, S.; Ozaki, Y. Submitted for publication.